

# Insulin-Like Growth Factor Binding Protein-3 (IGFBP-3) in the Prostate and in Prostate Cancer: Local Production, Distribution and Secretion Pattern Indicate a Role in Stromal-Epithelial Interaction

Petra Massoner,<sup>1</sup> Petra Haag,<sup>1</sup> Christof Seifarth,<sup>1</sup> Andreas Jurgeit,<sup>2</sup>  
Hermann Rogatsch,<sup>3</sup> Wolfgang Doppler,<sup>2</sup>  
Georg Bartsch,<sup>1</sup> and Helmut Klocker<sup>1\*</sup>

<sup>1</sup>Department of Urology, Innsbruck Medical University, Innsbruck, Austria

<sup>2</sup>Division of Medical Biochemistry of the Biocenter, Innsbruck Medical University, Innsbruck, Austria

<sup>3</sup>Department of Pathology, Innsbruck Medical University, Innsbruck, Austria

**BACKGROUND.** Insulin-like growth factor binding protein 3 (IGFBP-3) exerts inhibitory and proapoptotic effects on prostate cancer cells. Serum levels of IGFBP-3 were found to be associated with the risk of prostate cancer, but the data are still inconclusive. We present a detailed analysis of the expression and localization of IGFBP-3 in the prostate and a comparison with its expression pattern in tumors.

**METHODS.** Expression and localization of IGFBP-3 were analyzed in cellular models and tissue by real-time RT-PCR, ELISA, immunohistochemistry, and immunofluorescence.

**RESULTS.** All cell types of a panel of benign epithelial, stromal and tumor prostate cells expressed IGFBP-3. Significantly higher expression levels were registered in stromal cells. TGF- $\beta$  stimulation boosted IGFBP-3 levels 60-fold in stromal cells. The pattern of expression was confirmed in microdissected tissue samples. Protein levels measured by ELISA paralleled the mRNA levels and more than 80% of IGFBP-3 was secreted. On tissue immunostaining, IGFBP-3 was found to be mainly located in the epithelium. The pattern suggested secretion of IGFBP-3, which was confirmed in prostate tissue cultured *ex vivo* and the ejaculate of vasectomized men. IGFBP-3 levels were increased in primary tumors but did not differ from benign epithelium in metastases and local recurrent tumors.

**CONCLUSIONS.** We registered a significant local production of IGFBP-3 in the prostate, which may well override the effect of protein entering from blood. The stroma—particularly reactivated stroma—is the main source of IGFBP-3 in the prostate, suggesting that this peptide acts as a mediator of stromal-epithelial interactions. *Prostate* 68: 1165–1178, 2008.

© 2008 Wiley-Liss, Inc.

**KEY WORDS:** IGFBP-3; prostate cancer; stromal-epithelial interaction; expression; secretion

---

This article contains supplementary material, which may be viewed at the Prostate website at <http://www.interscience.wiley.com/jpages/0270-4137/suppmat/index.html>.

Grant sponsor: Cell Proliferation and Cell Death in Tumors; Grant number: SFB021; Grant sponsor: Austrian Research Foundation; Grant sponsor: PRIMA; Grant number: FP6-504587.

---

\*Correspondence to: Helmut Klocker, Department of Urology, Innsbruck Medical University, Anichstrasse 35, 6020 Innsbruck, Austria. E-mail: [helmut.klocker@uki.at](mailto:helmut.klocker@uki.at)

Received 3 December 2007; Accepted 1 April 2008  
DOI 10.1002/pros.20785

Published online 5 May 2008 in Wiley InterScience  
([www.interscience.wiley.com](http://www.interscience.wiley.com)).

## INTRODUCTION

Prostate cancer is one of the most frequently diagnosed malignancies and a common cause of cancer mortality in men in the Western hemisphere [1]. The progression of prostate cancer is a complex multistep process that starts with the transformation of normal cells and continues in terms of tumor growth, invasion and metastasis. It is now widely accepted that the promotion of carcinogenesis in the prostate depends on both, the epithelial and the stromal compartment. Transformed prostate epithelium and its surrounding stroma interact in a reciprocal manner, influencing each other due to multiple changes in their tissue micro-environment. The interaction between tumor and stroma culminates in the formation of a so-called reactive stroma. Reactive stroma is able to promote tumor proliferation and angiogenesis by growth factor expression and the migratory, invasive and metastatic behavior of tumor cells due to modification of the extracellular matrix [2–5].

Reducing mortality secondary to prostate cancer necessitates timely identification of risk factors and effective strategies for early diagnosis and curative treatment. Molecular approaches as well as genetic linkage studies are currently used to identify factors that increase the risk of developing prostate cancer and/or its progression.

One potential factor is the insulin-like growth factor binding protein-3 (IGFBP-3). However, published data concerning IGFBP-3 are contradictory. Whereas recent publications provide evidence of a positive association between IGFBP-3 and the risk of prostate cancer [6–9], previous case control studies have shown that high IGFBP-3 serum levels might exert a protective effect [10–13].

IGFBP-3 was shown to have multiple effects on cells by modulating cell growth and apoptosis via IGF-dependent and -independent mechanisms. IGFBP-3 is one of six members of the IGFBP family that non-covalently bind to IGFs with high affinity. The formation of IGF/IGFBP complexes prolongs the half-life of IGFs and increases their stability in the circulation. Thus, IGF/IGFBP complexes prevent interaction of IGFs with their specific receptors and block IGF-mediated proliferation and survival signals [14–16]. In addition to IGF-dependent actions, IGFBP-3 was shown to perform IGF-independent functions, including p53-dependent and independent pro-apoptotic functions [17,18]; anti-proliferative functions mediated by up-regulation of the cell cycle inhibitor protein p21/WAF1 [19]; and suppression of angiogenesis [20]. Various studies indicated that IGFBP-3 also acts as an anti-cancer molecule in prostate cancer [17,20–24].

Apart from its role as a risk factor, serum IGFBP-3 levels were investigated in respect of whether they might serve as a diagnostic or prognostic marker in addition to, or in combination with, the currently used prostate cancer marker PSA [7,25–27]. The established prostate cancer marker PSA is highly sensitive on one hand, and possesses low specificity on the other. The high false-positive rate of PSA [28] is a limitation that could be overcome by combining it with markers that better distinguish between cancer and benign disease. In the case of IGFBP-3 levels in serum, the results were ambiguous and not necessarily indicative of consistent improvement of cancer prediction [6–13].

To date, little is known about the local production of IGFBP-3 in the prostate although extensive efforts have been made to investigate the effects of exogenous IGFBP-3 on prostate cancer cells. Locally produced IGFBP-3 evidently acts on benign and malignant prostate cells and modulates, or even overrides, the effect of protein supplied from the blood. The aim of the present study was to collect data about the expression, location and secretion of IGFBP-3 in the prostate in order to elucidate its role in prostate cancer. Knowledge of the local production and bioavailability of IGFBP-3 is important in order to understand the biological effects of IGFBP-3 on prostate cells.

## MATERIALS AND METHODS

### Cell Culture

PC-3, Du145, and 22Rv1 were cultured in RPMI 1640 containing 10% fetal calf serum (FCS), 2 mM Glutamax (Invitrogen) and antibiotics. LNCaP were grown in MCDB-131 in the presence of 10% FCS, 2 mM Glutamax and antibiotics. LNCaP-abl and LNCaP-abl HOF cells were grown in MCDB-131 containing 10% charcoal-stripped FCS (CS-FCS), 2 mM Glutamax and antibiotics. The subline LNCaP-abl was established by maintaining LNCaP cells in steroid-depleted medium for 10 months. LNCaP-abl HOF cells were generated from LNCaP-abl cells which were grown as xenografts in nude mice and subsequently recultured [29–31]. Primary epithelial and stromal cell lines were taken from normal prostate tissue obtained from patients undergoing radical prostatectomy for prostate cancer, as previously described [32,33]. Immortalized prostate epithelium and stroma-derived cell lines were obtained by stable expression of hTERT [34]. All investigated cell lines are summarized in Table I.

### Treatment

Smooth muscle cells (SMC-T) immortalized by over-expression of human telomerase [34] were exposed to 10 ng/ml TGF- $\beta$  (Collaborative Biomedical Products)

**TABLE I. Cell Lines Characterized by Name, the Represented Cell Type, Cell Group, and Origin**

Name	Cell Type	Cell Group	Origin
PC-3	Metastatic PCa	Malignant epithelial	Prostate cancer bone metastasis
DU145	Metastatic PCa	Malignant epithelial	Prostate cancer brain metastasis
22Rv1	Metastatic PCa	Malignant epithelial	CWR22R xenograft line
LNCaP	Metastatic PCa, androgen sensitive	Malignant epithelial	Lymph node carcinoma of the prostate
LNCaP-abl	Metastatic PCa, castration resistant	Malignant epithelial	LNCaP, growing under steroid free conditions
LNCaP-abl HOF	Metastatic PCa, castration resistant	Malignant epithelial	LNCaP-abl xenograft
EP-1	Benign epithelial	Benign epithelial	Primary, deriving from normal prostate tissue
EP-2	Benign epithelial	Benign epithelial	Primary, deriving from normal prostate tissue
EP-T	Benign epithelial	Benign epithelial	EP, hTERT-immortalized
PF	Fibroblasts	Stroma	Primary, deriving from normal prostate tissue
SMC-1	Smooth muscle cells	Stroma	Primary, deriving from normal prostate tissue
SMC-2	Smooth muscle cells	Stroma	Primary, deriving from normal prostate tissue
SMC-T	Smooth muscle cells	Stroma	SMC, hTERT-immortalized

for 24 hr and collected for RNA isolation. Immortalized epithelial cells (EP-T) were treated with different amounts of human recombinant IGFBP-3 (kindly provided by Dr. Jansen-Dürr) and collected for Western Blot analysis.

#### Co-Culture

EP-T were cultured in the presence or absence of primary and immortalized stromal cells, respectively. The cells were grown as mixed cultures on 8 well-chamber slides (Nunc). On each slide 4 wells were used for growing co-cultures consisting of 1/3 epithelial and 2/3 stromal cells, whereas the remaining 4 wells were used for the respective single cultures. After 4 days of co-culture the cells were washed twice in PBS, fixed in 7% paraformaldehyde and analyzed for IGFBP-3 expression using immunofluorescent staining.

#### Ex Vivo Tissue Culture

Fresh tissue representing histologically normal areas was obtained from radical prostatectomy specimens and cut into 300- $\mu$ m sections using a Krumdieck precision tissue slicer (Alabama Research and Development Corporation). The tissue slices were loaded onto plastic grids in six-well plates containing culture medium (MCDB 153 supplemented with 1% FCS, 6 mM Glutamax and antibiotics). At pre-defined time points, 500  $\mu$ l of culture medium was sampled in order to determine IGFBP-3 protein concentration by ELISA, and replaced with fresh medium.

Representative tissue slices were fixed, embedded in paraffin, and cut into 7- $\mu$ m sections. Staining was performed using a Discovery XT automated immunohistochemistry system (Ventana Medical Systems) as described below in the immunohistochemistry section.

#### Tissue Microdissection

Frozen tissue sections of 10 radical prostatectomy specimens with histopathologically confirmed local prostate cancer scored according to Gleason (GSC 6, n=1; GSC 8, n=7; GSC 9, n=2) were cut into 8- $\mu$ m sections and mounted on sterile, RNase-free microscope slides. The slides were stained with hematoxylin and eosin for pathological analysis and exact localization of the tumors. Parallel unstained slides were used for microdissection. Slides for microdissection were pre-treated for 1 min in each of the following pre-cooled solutions: 75% ethanol, RNase-free water, 100% ethanol (twice) and xylene (twice). Before microdissection the slides were air-dried for 15 min. Benign and malignant epithelial areas, and stromal areas, were harvested separately. Laser-capture microdissection was performed on a Pix Cell II microdissection microscope (Arcturus) using 2,000–5,000 laser impulses to obtain tissue material for each RNA isolation. The size of the laser spot was 7.5  $\mu$ m<sup>2</sup> for epithelial cells and 30  $\mu$ m<sup>2</sup> for stromal cells. The intensity of the laser was 80 mW, 4.5 mA, 0.14 V, and the duration of the laser 2–8 msec. After microdissection the tissue was lysed in 50  $\mu$ l PicoPure extraction buffer (Arcturus) and stored at –80°C until it was used for RNA isolation.

#### RNA Isolation, Reverse Transcription, and Real-Time Polymerase Chain Reaction (PCR)

Total RNA from cell lines was isolated from 2 to 5 million cells using the RNeasy<sup>®</sup> Kit (Qiagen) according to the manufacturer's instructions. cDNA was generated from 1  $\mu$ g RNA using SuperScript<sup>™</sup> III reverse transcriptase (Invitrogen) and random hexamer primers.

RNA from microdissected cells was isolated using the PicoPure RNA isolation kit (Arcturus) according to the manufacturer's instructions. One sample consisting of isolated cells from 2,000 to 5,000 laser impulses was eluted in a final volume of 15  $\mu$ l elution buffer (Arcturus). RNA quantification and quality control were performed on a Bioanalyzer (Agilent). cDNA was generated from 5  $\mu$ l total RNA solution using SuperScript<sup>TM</sup> III reverse transcriptase (Invitrogen) and random hexamer primers.

Primer pairs and fluorescent probes for Taqman real-time PCR were designed according to sequences from the Nucleotide Sequence Database NCBI and ABI Prism Primer Express Software 2.0.0 (Applied Biosystems). All probes were synthesized spanning an exon-exon boundary and labeled with 5'FAM reporter dye and 3'TAMRA quencher dye. The following oligonucleotides were used: IGFBP-3 Forward: 5'-agcacagataccagaactctcc-3', Reverse: 5'-cattctctaccggcaggacc-3', Probe: 5'-ccgagtccaagcgggagacagaaatag-3' and TATA Box-binding protein (TBP) Forward: 5'-cacgaaccacggcactgatt-3', Reverse: 5'-tttctgtgctccagtctggac-3', Probe: 5'-tcttctcttggctctgtgcaca-3'. Real-time PCR was performed on an ABI Prism 7500 fast real-time PCR System (Applied Biosystems) using Taqman Universal PCR Mastermix (Applied Biosystems) according to the manufacturer's instructions. Primers and probes were used in a final concentration of 800 and 150 nM, respectively. Reactions were carried out in optical 96-well fast reaction plates (Applied Biosystems) in triplicate with 11  $\mu$ l reaction volume containing a maximum quantity of 25 ng of reverse-transcribed RNA. Newly designed primer-probe pairs were tested by amplification of a five-step 10-fold dilution series of standardized cDNA and by comparing the resulting slopes. The corresponding efficiencies were calculated according to the equation  $E = 10^{(-1/\text{slope})}$ . The used systems were characterized as follows: IGFBP-3 slope, -3.21;  $R^2$ , 0.992; PCR efficiency, 2.049; TBP slope, -3.27;  $R^2$ , 0.997; PCR efficiency, 2.027. Relative quantification was performed by comparing  $dC_t$  values achieved by normalization of cycle threshold ( $C_t$ ) values of IGFBP-3 to  $C_t$  values of TBP as endogenous expression control, using the following formula:  $2^{-dC_t} = 2^{-(C_t \text{ IGFBP-3} - C_t \text{ TBP})}$  [35-37].

### IGFBP-3 Sandwich ELISA

IGFBP-3 protein concentrations in cell pellets, cell and tissue culture supernatant as well as in ejaculates of vasectomized men were quantified using human IGFBP-3 sandwich ELISA (R&D Systems) according to the manufacturer's instructions. The samples were collected as follows. Twenty-three ejaculate samples of patients undergoing medical examination after

vasectomy were collected and stored at  $-20^\circ\text{C}$  until they were used for measurement. Prior to measurement the samples were thawed only once and used directly for serial dilutions in reagent diluent for ELISA (5% Tween<sup>®</sup> 20, 2% normal goat serum in PBS).

Cells were cultured over 4 days. Cell culture supernatants and cells were harvested separately. Cell numbers were determined using the CASY cell counter and analyzer system (Schärfe System, Reutlingen, Germany). Cell pellets were washed in PBS and lysed in buffer containing 20 nM  $\text{NaH}_2\text{PO}_4$  (pH 7.5), 1 mM ethylenediaminetetracetic acid (EDTA), 10% glycerol, 1 mM phenylmethylsulfonyl fluoride (PSMF), 5 mM sodium fluoride (NaF), protease inhibitors (Calbiochem) and phosphatases inhibitors (Sigma-Aldrich). Serial dilutions of cell lysates were made in reagent diluent for ELISA, starting with equal protein concentrations (determined by Bradford's method). Cell and tissue culture supernatants were used directly for dilutions in reagent diluent for ELISA.

For all measurements, cell culture medium, FCS and reagent diluent were used as negative controls whereas human serum served as positive control.

### Western Blot Analysis

Cell pellets and ejaculate samples were lysed in  $2\times$  Glycine SDS sample buffer (Gradipore) and total protein was quantified using the Bradford method. 20 (cell-extracts) or 50 (ejaculate samples)  $\mu$ g of protein per lane were then resolved using a 4-12% Bis-Tris gel (Invitrogen) and transferred onto a nitrocellulose membrane (Invitrogen). The membrane was blocked for 1 hr using Starting Block (TBS) buffer (Pierce Biotechnology) and incubated at  $4^\circ\text{C}$  overnight with an anti-IGFBP-3 antibody (DSL, 1:1,000) and an anti-GADPH antibody (Chemicon, 1:10,000) used as loading control. This step was followed by incubation for 1 hr at room temperature with fluorescence-labeled secondary antibodies (Molecular Probes). The membranes were scanned using the Odyssey infrared imaging system and densitometric analysis was performed using Odyssey application software (LiCor Biosciences).

### Immunohistochemistry

Tissue sections of 26 primary prostate cancer samples of Gleason scores 6-9 (GSC 6,  $n=8$ ; GSC 7,  $n=10$ ; GSC 9,  $n=8$ ), 22 samples of local recurrent tumors after failure of androgen ablation therapy, and 16 tissue samples of lymph node and distant metastasis, were collected and embedded in paraffin. Tissue blocks were cut into 5- $\mu$ m sections. Antigen retrieval and immunohistochemistry were performed using a Discovery XT automated immunohistochemistry

system (Ventana Medical Systems). All tissue sections were pre-treated according to standard cell conditioning, which consisted of heat retrieval at 100°C for 30 min in cell conditioning solution CC1 buffer pH 9.0 (Ventana Medical Systems). Primary antibodies were diluted 1:100 and incubated for 1 hr at 37°C, followed by iView DAP MAP detection (Ventana Medical System) and hematoxylin counterstaining. IGFBP-3 was stained using either a rabbit polyclonal (Upstate Biotechnology) or a mouse monoclonal antibody (R&D Systems) to prove the accuracy of the staining. The cell proliferation marker Ki-67 was stained using a mouse monoclonal antibody (DAKO). Controls consisted of mouse and rabbit universal negative controls (Dako-Cytomation). Semi-quantitative grading of stained tissue sections was performed by a pathologist; the number of positive cells and the staining intensity were taken into account. A Quick score method such as that described for estrogen receptor [38] was used to classify the samples. A five-step grading system ranging from 0 (negative) to 4 (positive) was used for the classification. Images were captured using the Axio Imager M1 (Zeiss) and the Pixelink Capture OEM (Pixelink) image acquisition program.

#### Immunofluorescent Staining

Immunofluorescent staining was performed on six representative primary prostate cancer samples collected for immunohistochemistry and on co-cultures established on 8-well chamber slides. Tissue sections were deparaffinized in xylol and rehydrated in a graded series of alcohol. Antigen retrieval was per-

formed by heating samples in Tris-EDTA buffer to 120°C for 10 min (Decloaking Chamber, Biocare Medical). Slides were blocked in PBS containing 0.2% Triton X-100 and 10% normal goat serum for 30 min at 37°C. Co-culture chamber slides subjected to blocking without antigen retrieval. Primary antibodies were diluted 1:100 in PBS containing 0.2% Triton X-100 and 2% normal goat serum, and incubated for 1 hr at 37°C. For immunofluorescence we used the same antibodies as those used for immunohistochemistry to detect IGFBP-3. Cytokeratin 8 was stained using a mouse monoclonal antibody (Abcam). After washing the slides in PBS, secondary Alexa Fluor 488 and/or Alexa Fluor 555-conjugated donkey or goat anti-rabbit, mouse antibodies (Invitrogen) were added for 30 min at 37°C, followed by another extensive washing step in PBS. Nuclear counterstaining was performed optionally by incubating the slides in a 25-nM SYTOX green solution (Invitrogen) in PBS for 5 min or using mounting medium containing 4,6-diamidino-2-phenylindole (DAPI). All samples were covered with Vectashield mounting medium (Vector Laboratories). Images were captured using a Zeiss Axiovert 200 equipped with a LSM510 META detector (Zeiss). Cross talk between fluorescent channels was checked with single dye treated samples.

Immunofluorescent staining of co-cultures was quantified using TissueQuest immunohistochemistry analysis software (TissueGnostics, Vienna). A detailed description of the analysis is provided in supplementary Figure 1. Cytoplasmatic staining intensity of IGFBP-3 in cytokeratin positive epithelial cells cultured

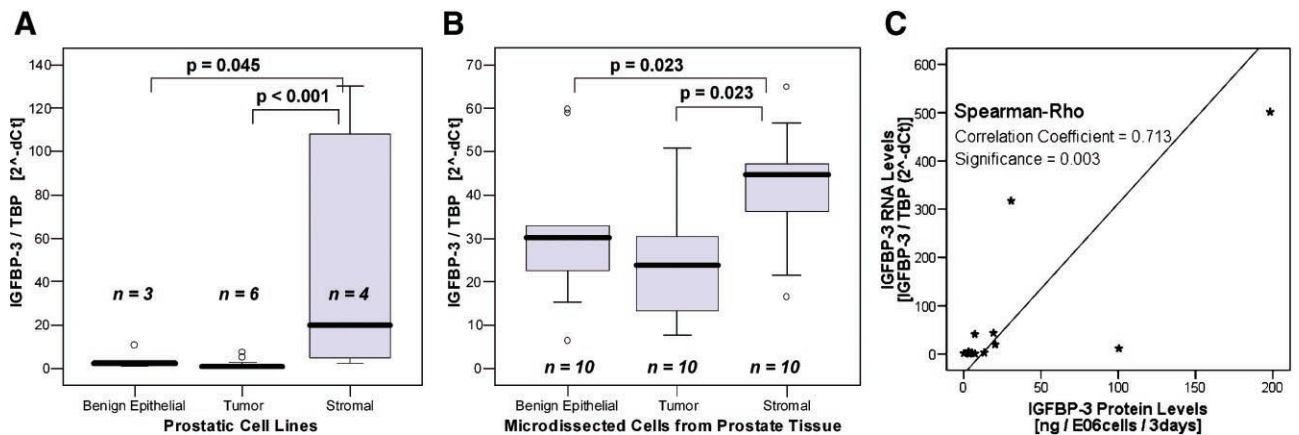


**Fig. 1.** IGFBP-3 expression in the prostate: The Y-axis shows relative IGFBP-3 mRNA concentrations compared to the endogenous control TATA Box binding protein ( $2^{-\Delta\Delta Ct}$ ). **A:** IGFBP-3 expression in prostatic cell lines. RNA was isolated from a panel of benign and malignant prostate cell lines as listed in Table I, and IGFBP-3 expression was measured in three independent experiments by Taqman real-time PCR. Stromal cells had significantly greater quantities of IGFBP-3 mRNA than did benign and malignant epithelial cells. **B:** IGFBP-3 expression in microdissected cells derived from prostate tissue. Frozen sections of 10 radical prostatectomy specimens were microdissected. RNA was isolated from benign epithelial, tumor and stromal cells, and subjected to real-time PCR analysis. Again, significantly larger quantities of IGFBP-3 mRNA were found in stromal cells than in benign and malignant epithelial cells. **C:** Significant correlation (correlation coefficient 0.7;  $P = 0.003$ ) of IGFBP-3 mRNA expression with IGFBP-3 protein levels in prostatic cell lines. IGFBP-3 protein levels were measured using sandwich ELISA.

in the presence or absence of different types of stromal cells was calculated.

### Statistics

Statistical calculations were performed using SPSS 12.0 for Windows. The Kolmogorov–Smirnov test was used to investigate normal distribution of data sets. Considering the fact that nearly all data (except cell culture data) were non-normally distributed, Spearman's Rho test was used to calculate the correlation coefficients while the Mann–Whitney *U*-Test was employed to analyze the significance of differences in various cell and patient groups. Wilcoxon's test was performed to establish differences in IGFBP-3 expression and accumulation in benign and malignant cells of the same tissues, considering that these data represent matched-sample pairs. Medians and interquartile ranges are presented for non-normally distributed data, whereas means and standard deviations are presented for normally distributed data. *P* values below 0.05 were considered significant and displayed as exact values when  $\geq 0.001$ .

### Diagrams

Box blot diagrams were used for visual description of different datasets. The bold line in box blots represents the median score while the bottom and top of the boxes represent the first and the third quartiles, respectively. Range bars indicate lowest and highest scores. Outliers are marked with open circles.

## RESULTS

### IGFBP-3 Expression in Benign and Malignant Prostatic Cell Lines

We first investigated which prostatic cells are able to produce IGFBP-3 and the expression levels in the different cell types. Total RNA was isolated from a panel of epithelial and stromal benign cell lines and a set of tumor cell lines representing the different stages of prostate cancer. We detected IGFBP-3 mRNA by real-time PCR in all investigated cell lines and calculated the expression levels using the housekeeping gene TATA-box binding protein (TBP) as reference. As shown in Figure 1A, stromal cells were the main producers of IGFBP-3 ( $2^{-dCt}$  median, 20; interquartile range (IQR), 110). Stromal cells contained 10-fold more IGFBP-3 mRNA than did benign epithelial cells ( $2^{-dCt}$  median, 2.1; IQR, 6.1;  $P = 0.045$ ) and 20-fold more IGFBP-3 mRNA than did prostate cancer cells ( $2^{-dCt}$  median, 0.7; IQR, 1.84;  $P < 0.001$ ).

In order to determine whether mRNA is correlated with protein levels of IGFBP-3 we measured IGFBP-3 protein levels using sandwich ELISA. IGFBP-3 mRNA

expression was significantly correlated with protein levels (correlation coefficient = 0.71;  $P = 0.003$ ; Fig. 1C). Cells containing large quantities of IGFBP-3 mRNA also produced the largest quantities of protein. After 4 days of culture, 80–98% of all produced IGFBP-3 protein were found in the cell culture supernatant, confirming that the protein was secreted after production.

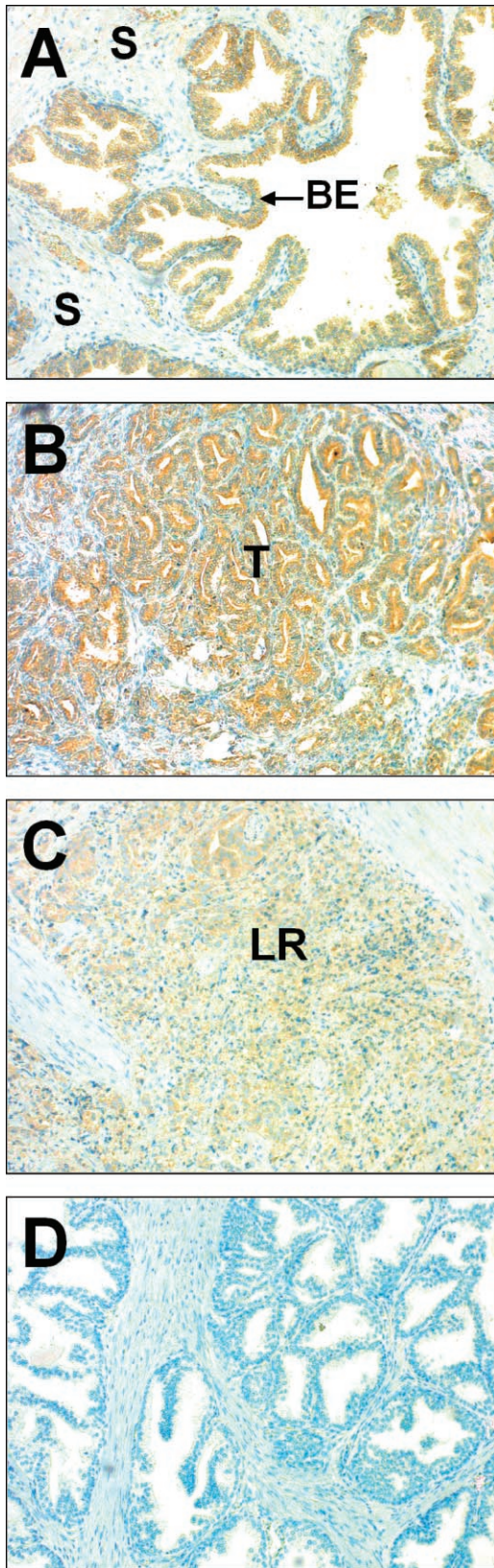
These results show that IGFBP-3 is expressed by all prostatic cell lines. Stromal cells produced the largest quantities of IGFBP-3 protein while all cells secreted the protein after production.

### IGFBP-3 Expression in the Human Prostate

In order to investigate whether IGFBP-3 expression in prostatic cell lines reflects the situation in human prostate tissue, we measured IGFBP-3 mRNA levels in prostatic cells isolated by laser capture microdissection. Human prostate specimens were obtained from patients undergoing radical prostatectomy after prostate cancer had been confirmed in a PSA-based screening program. As shown in Figure 1B, we detected IGFBP-3 mRNA by real-time PCR in all investigated samples. The expression pattern in the tissue was similar to that observed in cell lines. Again, IGFBP-3 expression was higher in stromal cells ( $2^{-dCt}$  median, 44.7; IQR, 17.2) than in benign epithelial cells ( $2^{-dCt}$  median, 30.1; IQR, 18.5;  $P = 0.023$ ) and epithelial cells from local tumors ( $2^{-dCt}$  median, 23.9; IQR, 17.4;  $P = 0.023$ ). IGFBP-3 expression was not significant different between malignant and benign epithelial cells. This experiment shows that IGFBP-3 is locally produced in the prostate, and the stroma is the principal site of local IGFBP-3 production.

### IGFBP-3 Localization in the Human Prostate

IGFBP-3 protein in human prostate tissue was detected by immunohistochemistry and immunofluorescent staining. The protein was mainly located in epithelial cells. Although stromal areas were also positive for IGFBP-3, they never achieved the staining intensity of the epithelia (Fig. 2). The accuracy of immunohistochemistry was confirmed using two antibodies: a mouse monoclonal and a rabbit polyclonal antibody were used to identify IGFBP-3 (supplementary Fig. 2) while commercial rabbit and mouse monoclonal control antibodies were used as negative controls. With both antibodies we observed the same IGFBP-3 distribution. Neither control antibodies yielded staining, indicating that IGFBP-3 detection in the prostate was, indeed, specific. The epithelial localization of IGFBP-3 was confirmed by immunofluorescent double-staining with cytokeratin 8, a marker for epithelial cells (Fig. 3), and was consistent



with previous reports showing IGFBP-3 immunoreactivity in prostatic epithelia [39–41]. A more detailed investigation (Fig. 4) showed that IGFBP-3 was located in vesicular structures, which were distributed all over the epithelium and in some stromal areas.

In summary, we found that IGFBP-3 protein in the prostate is predominantly located in epithelial cells.

#### IGFBP-3 Localization in Prostate Cancer

We next investigated whether there are differences in IGFBP-3 levels between benign prostate and prostate cancer. IGFBP-3 immunohistochemistry analysis was performed on 27 tissue samples of local tumors, 22 tissue samples of locally recurrent tumors, and 16 samples of metastatic disease. We observed a greater intensity of IGFBP-3 staining in local tumors compared to benign epithelial cells of the same tissue ( $P = 0.001$ ), indicating that cancer cells possess larger quantities of IGFBP-3 (Table II). However, the increase in IGFBP-3 staining was not correlated with the pathological stage or grade of these tumors (supplementary Table I). The IGFBP-3 content of recurrent tumors and metastatic lesions was similar to that of benign epithelial cells. Thus, there was significantly lower immunoreactivity at these sites compared to local malignancies ( $P = 0.012$  and  $P = 0.001$ ). Lymph node and distant metastases were marked by similar levels of staining intensity.

These data show that IGFBP-3 protein levels in local tumors are higher than those in benign tissues as well as recurrent tumors and metastatic lesions of the prostate.

#### IGFBP-3 Secretion of Prostatic Tissue

Immunofluorescent and immunohistochemical studies revealed that IGFBP-3 protein is present in epithelial cells of the prostate. We therefore hypothesized that the protein may be secreted from prostate tissue. To investigate this hypothesis we performed an ex vivo culture of prostatic tissue and observed whether IGFBP-3 was secreted from the cultured tissue into the surrounding medium. The experiment was performed for three representative tissues which were cultured over a period of 7 days. In all the three tissue cultures we observed a constant increase of IGFBP-3 in the tissue culture medium (ELISA measurement,

**Fig. 2.** Immunolocalization of IGFBP-3 in benign human prostate and prostate cancer. IGFBP-3 detected by immunohistochemistry was mainly located in epithelial cells of benign (A) and malignant (B,C) portions of the prostate. Local tumors (B) showed greater IGFBP-3 staining than did benign epithelia (A) and local recurrent tumors (C). See Table II for scoring results. D: Isotype control. Blue counterstaining was done with hematoxylin. Magnification: 100-fold. BE, benign epithelium; S, stroma; T, local tumor; LR local recurrent tumor.

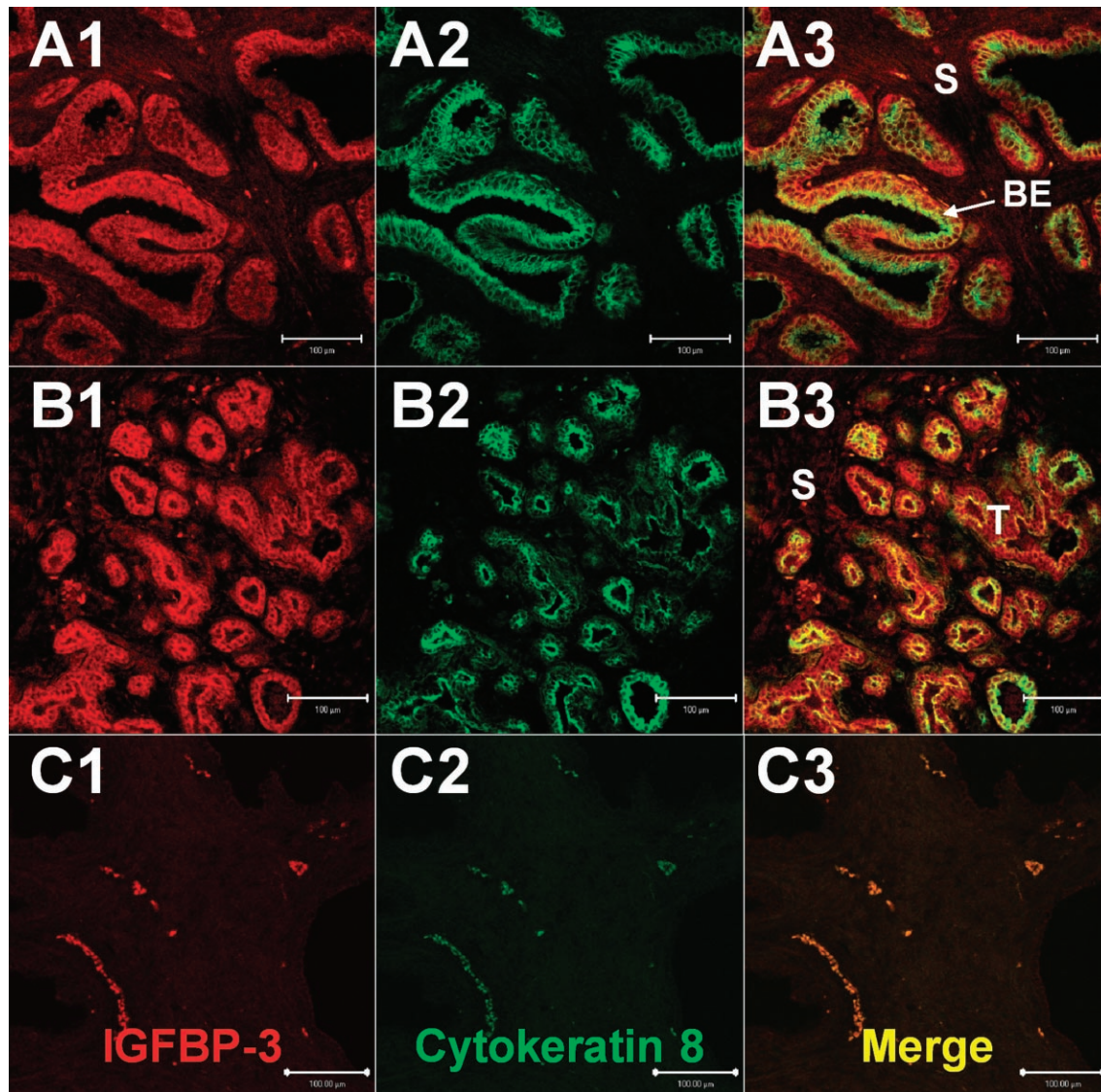


**Fig. 3.** Immunofluorescent co-staining of IGFBP-3 (red) and cytokeratin 8 (green) in the prostate. IGFBP-3 was located in cytokeratin-8-positive benign (A) and malignant (B) epithelial cells. Stromal areas were also IGFBP-3 positive but their staining intensity was lower. IGFBP-3 was stained in red using an ALEXA 555-labeled secondary antibody (A1–C1) whereas cytokeratin 8, a marker for epithelial cells, was stained in green using an ALEXA 488-labeled secondary antibody (A2–C2). Merging the two channels is shown in A3–C3. Staining with an isotype control (C) ensured specificity. Positive events in the negative control were identified as erythrocytes because of their typical shape and negative DAPI staining (data not shown). White bars represent 100 µm. BE, benign epithelium; T, tumor areas; S, stroma.

Fig. 5B). These data show that IGFBP-3 is consistently secreted from prostatic tissue. To further investigate this phenomenon we stained representative tissue slices from cultured tissue for IGFBP-3 and the proliferation marker Ki-67 using immunohistochemistry (Fig. 5A). IGFBP-3 staining in tissue prior to tissue culture (day 0) showed the characteristic IGFBP-3 staining seen in normal prostate tissue: The protein was mainly located in epithelial cells whereas stromal areas showed only weak IGFBP-3 immunoreactivity. After 7 days of tissue culture (day 7), a remarkable change was observed: IGFBP-3 staining in

stromal areas was significantly increased while the staining intensity in epithelial compartments remained the same. When we investigated tissue proliferation using the proliferation marker Ki-67 we detected at day 0 only a few proliferating cells. After 7 days of tissue culture the proportion of Ki-67 positive cells was markedly increased. Ki-67 positive cells were mainly located in the epithelium. In parallel, IGFBP-3 production in stromal areas is up-regulated during culture.

To confirm the secretion of IGFBP-3 by the prostate gland we analyzed ejaculate samples of 23 vasectomized men. The ejaculate samples contained

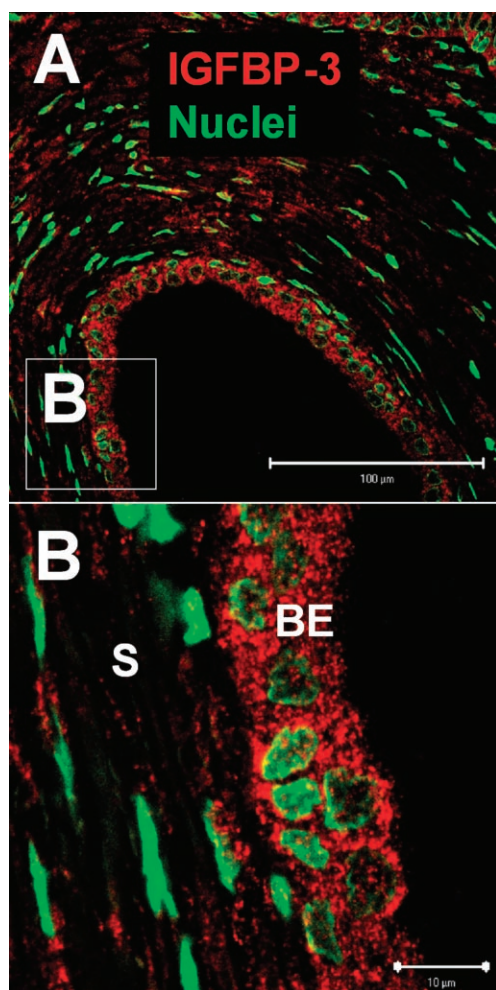


**Fig. 4.** Cellular localization of IGFBP-3 using confocal microscopy. IGFBP-3 was stained in red, nuclear counter-staining was achieved by SYTOX green. **A:** In the normal human prostate, IGFBP-3 showed enhanced accumulation in epithelial cells. **B:** Enlarged section of (A). In a detailed view IGFBP-3 was found in vesicular structures distributed all over the epithelium. White bars represent 100  $\mu\text{m}$  in A and 10  $\mu\text{m}$  in B. BE, benign epithelium; S, stroma.

a large quantity of prostatic secretion because testicular fluid is not present after vasectomy. IGFBP-3 was detected in 90% of all investigated samples (median, 142 ng/ml; IQR, 677 ng/ml) when using ELISA. In addition, the samples were subjected to Western Blot analysis. A representative Western Blot is shown in Figure 5C. In summary these data show that IGFBP-3 is secreted by prostatic tissue and can be found in ejaculate. In ex vivo prostate tissue cultures, IGFBP-3 is up-regulated in stromal compartments.

#### IGFBP-3 Levels in Epithelial Cells are Influenced by Stromal Cells

We next investigated whether the presence of IGFBP-3 in the extra-cellular environment of epithelial

cells can influence their intracellular IGFBP-3 content. We exposed immortalized epithelial cells (EP-T) to human recombinant IGFBP-3 for 24 hr and measured their intracellular IGFBP-3 level by Western Blot analysis. The cells were treated with trypsin and washed in PBS prior to sample collection in order to avoid that any protein attached to the membranes was included in the analysis. We observed a dose dependent increase in the intracellular IGFBP-3 content of epithelial cells when they were exposed to increasing amounts (100–2,000 ng/ml) of recombinant IGFBP-3 (Fig. 6A). This demonstrates the ability of epithelial cells to take up IGFBP-3 from their environment.

We next elucidated whether stromal cells are able to influence the intracellular IGFBP-3 content of epithelial cells. We co-cultured epithelial and stromal cells as described under material and methods and stained for IGFBP-3 and the epithelial cell marker cytokeratin 8 using immunofluorescent staining techniques (Fig. 6B). IGFBP-3 staining intensity of cytokeratin positive epithelial cells was calculated using TissueQuest immunofluorescence analysis software (supplementary Fig. 1). The results show that epithelial cells cultured in the presence of stromal cells contain up to 2.3-fold more IGFBP-3 than epithelial cells grown as single cultures (Fig. 6C). The effect was more pronounced when primary cultures of stromal cells were used for the experiments instead of immortalized cultures. These results show that stromal cells in contact to epithelial cells can significantly influence the intracellular IGFBP-3 content of epithelial cells.

#### TGF- $\beta$ Up-Regulates IGFBP-3 in Stromal Cells

Our immunohistochemistry data show an increase of IGFBP-3 protein in local tumors of the prostate when compared with benign tissue. As discussed below, we consider the stroma to be the main source of IGFBP-3 in local tumors. TGF- $\beta$  was described to be one of the key factors involved in the carcinoma-induced stromal response [2,3] and was shown to up-regulate IGFBP-3 in the prostate cancer cell line PC3 [17].

In order to determine whether TGF- $\beta$  influences IGFBP-3 in stromal cells we exposed immortalized smooth muscle cells (SMC-T) to 10 ng/ml TGF- $\beta$  for 24 hr and investigated IGFBP-3 mRNA levels using real-time PCR. This treatment boosted IGFBP-3 mRNA 60-fold compared to control cells ( $2^{-\text{dCt}}$  mean, 2.96; standard deviation, 0.5 vs. mean, 194.1; standard deviation, 13.25;  $P < 0.001$ ; Fig. 7).

#### DISCUSSION/COMMENTS

IGFBP-3 has been frequently discussed as a tumor-inhibiting protein for prostate cancer. However, it has also been described as a potential serum marker for

**TABLE II. Semiquantitative Analysis of IGFBP-3 Immunoreactivity in Benign Epithelium, Local Tumors, Hormone-Refractory Tumors, and Metastatic Lesions of the Prostate**

IGFBP-3 staining score	Positive n/total (%)			
	BE	LT	LR	ME
0	00/27 (0.00)	01/26 (03.8)	00/22 (00.0)	03/16 (18.8)
1	00/27 (0.00)	00/26 (00.0)	06/22 (27.3)	04/16 (25.0)
2	13/27 (48.1)	00/26 (00.0)	01/22 (04.5)	00/16 (00.0)
3	12/27 (44.5)	12/26 (46.2)	10/22 (45.5)	09/16 (56.2)
4	02/27 (07.4)	13/26 (50.0)	05/22 (22.7)	00/16 (00.0)
<i>P</i> -value	0.001 (BE vs LT)			
	0.012 (LT vs LR)			
	0.001 (LT vs ME)			

Immunohistochemistry was performed according to a standard horseradish peroxidase staining protocol and immunoreactivity was scored by a pathologist. Local tumors showed strong IGFBP-3 staining more frequently than did benign epithelial cells of the same tissue ( $P=0.001$ ). Locally recurrent tumors after hormone therapy as well as metastatic lesions showed less IGFBP-3 staining than did primary local tumors ( $P=0.012$  and  $P<0.001$ ). IGFBP-3 immunohistochemistry staining was graded into five categories ranging from 0 (negative) to 4 (positive) as described in the Materials and Methods section.

BE, benign epithelia; LT, local tumors; LR, locally recurrent tumors; ME, metastases.

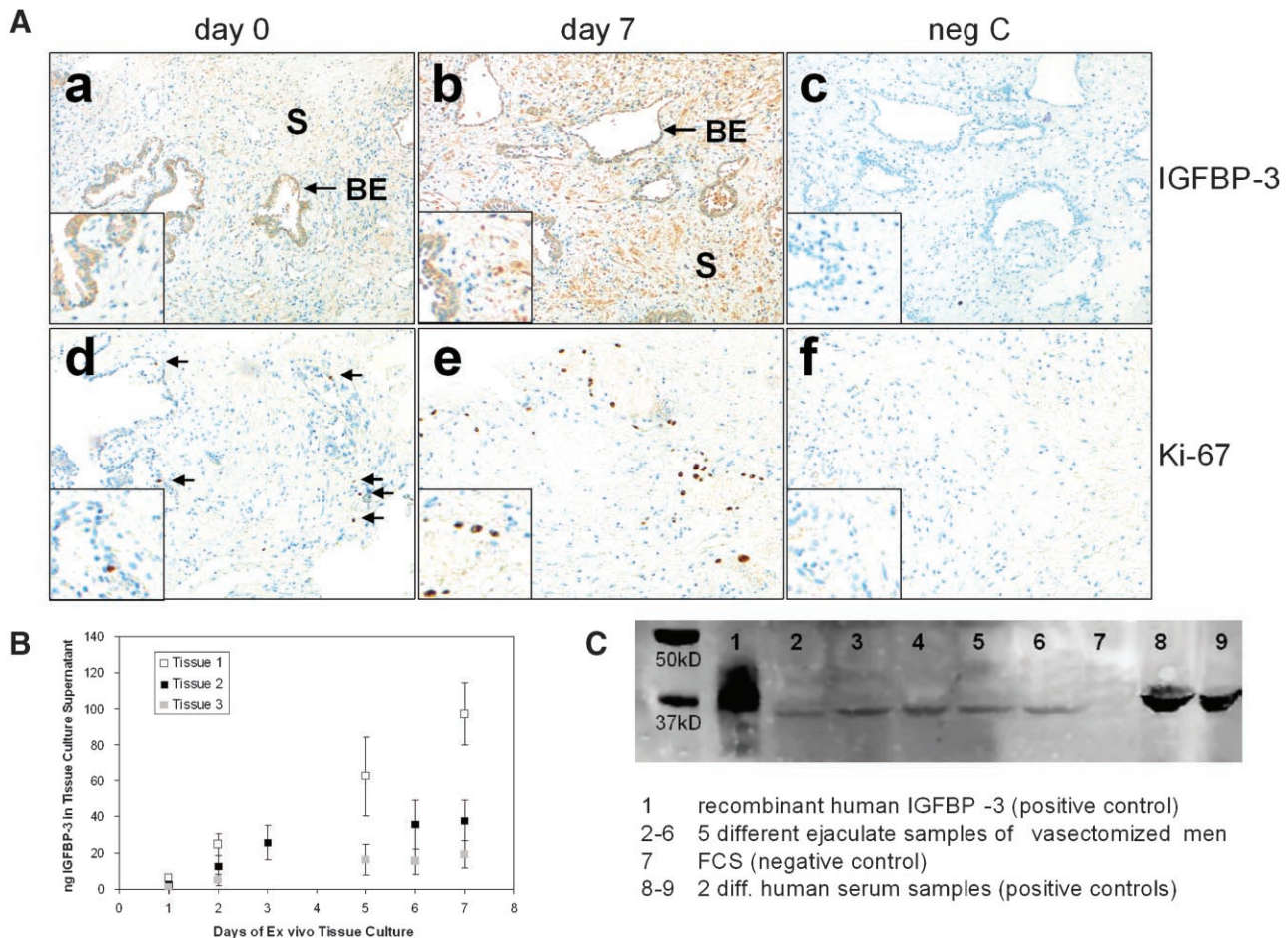


**Fig. 5.** IGFBP-3 secretion of prostatic tissue. Prostate tissue sections were cultured ex vivo for 7 days and release of IGFBP-3 into the supernatant was measured using a sandwich ELISA. The release of IGFBP-3 into prostatic secretions was confirmed by detection of IGFBP-3 in ejaculates of vasectomized men. **A:** Immunohistochemical staining of IGFBP-3 (**a, b**) and the proliferation marker Ki-67 (**d, e**) in prostate tissue cultured ex vivo. **a, d:** Tissue after radical prostatectomy (day 0). **b, e:** Tissue cultured ex vivo for 7 days (day 7). **c, f:** Staining control using an isotype control antibody (neg. C, day 7). Magnification: 100-fold, Detail: 200-fold. BE, benign epithelium; S, Stroma. **B:** IGFBP-3 secretion into the supernatant of three representative prostate tissues cultured ex vivo (ELISA measurement). **C:** Detection of IGFBP-3 protein in ejaculate samples of vasectomized men (immunoblot).

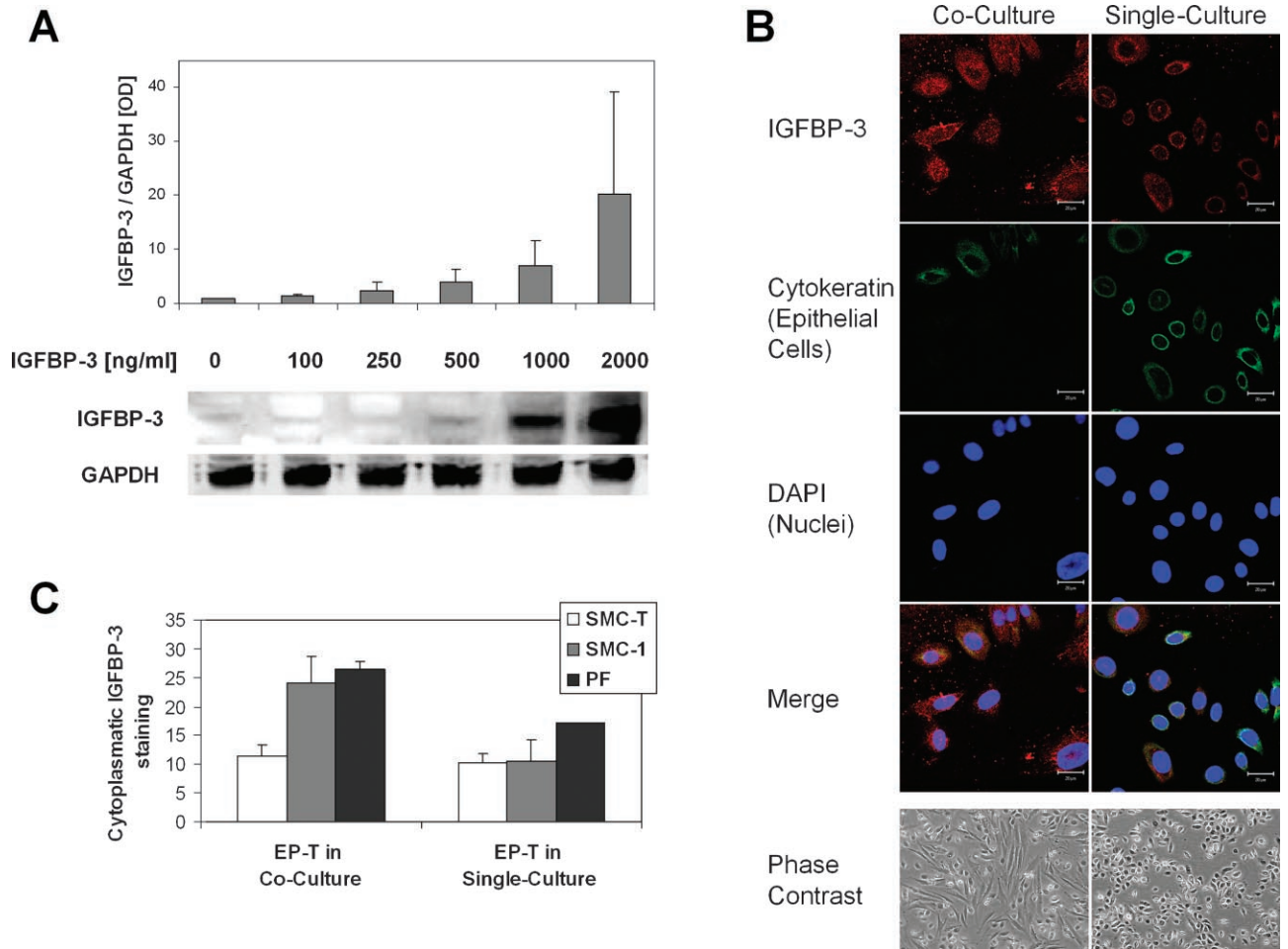


**Fig. 6.** Intracellular IGFBP-3 levels in prostate epithelial cells increase after treatment with recombinant IGFBP-3 or co-culture with stromal cells. **A:** Immortalized prostate epithelial cells (EP-T) were treated with different amounts of IGFBP-3 for 24 hr. Intracellular IGFBP-3 levels were measured by immunoblot and normalized against GAPDH. **B:** EP-T cells were cultured in the presence (co-culture) or absence (single culture) of stromal cells. IGFBP-3, cytokeratin 8, a marker for epithelial cells and the nuclei(DAPI) were visualized by immunofluorescent staining. Images were taken using a confocal microscope (magnification 40 -fold), phase contrast images with a conventional microscope (magnification 4-fold). **C:** Epithelial cells (EP-T) cultured in the presence of stromal cells (co-culture) contained higher amounts of IGFBP-3 than EP-T cultured as single cultures. Three different stromal cell lines were used: immortalized stromal cells (SMC-T), primary smooth muscle cell-like stromal cells (SMC-1) and primary fibroblast-like smooth muscle cells (PF). Cytoplasmic immunofluorescent staining of IGFBP-3 in EP-T cultured in the presence or absence of primary and immortalized stromal cells (Table I) was quantified using TissueQuest analysis software.

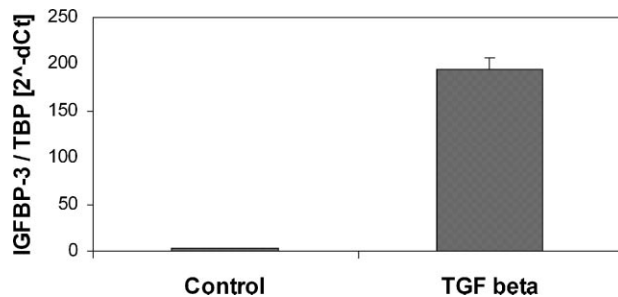


**Fig. 7.** Transforming growth factor beta (TGF)-can up-regulate IGFBP-3 in prostate stromal cells. Immortalized smooth muscle cells (SMC-T) were exposed to 10 ng/ml TGF-for 24 hr. IGFBP-3 mRNA was measured using real-time PCR. n = 3; P < 0.001.

prostate cancer. Epidemiologic studies correlating serum IGFBP-3 levels with the risk and development of prostate cancer failed to show consistent results [6–13,42].

One reason for this inconsistency could be the contribution of different sites of local IGFBP-3 production, in terms of tissues as well as cell types. The major part of circulating IGFBP-3 in the human body is believed to originate in the liver [43,44]. Local production of IGFBP-3 occurs in significant measure in the prostate. It also appears to be secreted into prostatic fluid. Serum IGFBP-3 therefore does not reflect the effects of IGFBP-3 in the prostate and may also not reflect disease-related alterations in prostatic IGFBP-3

levels. Locally produced IGFBP-3 may modulate or even outweigh the influence of serum IGFBP-3 in the prostate. In view of these facts, it is obviously difficult to correlate serum IGFBP-3 with the prognosis of prostate cancer.

This study was undertaken to identify sites of local production of IGFBP-3 in the prostate and its potential contribution to prostate cancer. We showed that, in the prostate gland, IGFBP-3 is locally expressed by different cell types in different quantities. The large part of IGFBP-3 is produced by stromal cells. This was an unexpected finding considering that IGFBP-3 was predominantly located in epithelial cells, as shown in this study as well as by others [39–41]. In cell culture experiments, most of the IGFBP-3 was secreted after its production. We therefore hypothesized that prostatic IGFBP-3 is mainly produced by the stroma and, after secretion, is taken up by epithelial cells. Epithelial cells cultured either in the presence of stromal cells or exposed to extra-cellular human recombinant IGFBP-3 contained indeed higher amounts of the protein than control cells. Similar observations were made in respect of IGFBP-5, a further IGF-binding protein produced in the prostate. Tennant et al. [45] showed that the IGFBP-5 mRNA signal detected by *in situ* hybridization in prostatic tissue was located all over stromal cells while IGFBP-5 immunoreactivity was high in epithelial cells. This led to the conclusion that IGFBP-5 produced by stromal cells is sequestered by epithelial cells. A similar distribution of mRNA and protein was observed for IGFBP-3, suggesting that IGFBP-3 behaves in a similar manner. The stroma as a source of IGFBP-3 in the prostate is a new observation that may be of great relevance in understanding how IGFBP-3 exerts its biological effects on epithelial cells.

We registered an increased level of IGFBP-3 protein in local adenocarcinoma of the prostate when comparing the samples with benign tissue using immunohistochemistry. This finding was in contrast to previous studies which described a down-regulation of IGFBP-3 in prostate cancer [40,46]. Interestingly, comparison of our data obtained by real-time PCR and by immunohistochemistry showed that increased quantities of IGFBP-3 protein in local tumors were not associated with increased expression of IGFBP-3 in tumor cells. This would suggest that the increased levels of IGFBP-3 in malignant epithelial cells of local tumors result from the uptake of IGFBP-3 derived from the tumor surrounding stroma.

Our observation, that stromal IGFBP-3 is rising in tissue cultured *ex vivo*, would support this hypothesis. Tissues kept in culture are exposed to a change in their microenvironment, which may lead to activation of the tissue. After 7 days of culture we observed greater tissue proliferation determined by Ki-67 staining. In

addition stromal IGFBP-3 was dramatically increased, suggesting that the activation of stromal tissue had led to an up-regulation of IGFBP-3.

Tissue cultured *ex vivo* may be activated by altered conditions resulting from the culture. In the human body a change in the tissue microenvironment can be induced when a tumor develops within the tissue, leading to a functional epithelial and stromal response [3,4]. Considerable evidence points to TGF- $\beta$  as one of the key mediators of carcinoma-induced stromal response [2,3]. Stromal activation due to tumor development may also be expected to increase IGFBP-3 production. We therefore investigated whether TGF- $\beta$  was able to up-regulate IGFBP-3 in stromal cells and found a dramatic up-regulation of IGFBP-3 mRNA when prostate smooth muscle cells were exposed to TGF- $\beta$ .

These findings give rise to the following hypothesis: Tumors alter the microenvironment of prostate tissue. TGF- $\beta$  and other auto- and paracrine factors lead to a stromal response, causing a change in the stromal expression profile and, amongst other phenomena, up-regulation of IGFBP-3. IGFBP-3 is secreted into the extracellular matrix and can be taken up by neighboring cells, including epithelial cells. As a result, the IGFBP-3 content of malignant epithelial cells in local tumors is greater than that of benign epithelial cells. In accordance with our hypothesis, locally recurrent tumors and metastases of the prostate, which are characterized by a diminished stromal support, did not show an increase in IGFBP-3 protein levels. The influence of the stroma on the bioavailability of IGFBP-3 in the prostate and in prostate cancer would be a new mechanism by which the stroma is able to influence tumor biology. Further research will be needed to elucidate the effects of the stroma in modulating IGFBP-3 bioavailability, and to determine the role of this influence in tumor biology and tumor progression.

The elevated quantities of IGFBP-3 we observed in epithelial cells surrounding prostatic ducts indicate that IGFBP-3 is released into prostatic fluid. This hypothesis was confirmed by the detection of secreted IGFBP-3 in culture media of *ex vivo* cultures of prostate tissue and the presence of IGFBP-3 in the ejaculate of vasectomized patients. As the testes do not contribute to the ejaculate in vasectomized patients, the main part of the IGFBP-3 detected here is probably derived from the prostate. It should be noted that prostate-derived IGFBP-3 levels in ejaculate might be underestimated due to degradation of IGFBP-3 by PSA and other proteases [47,48]. This is also reflected by the large differences in IGFBP-3 concentrations between the investigated samples.

In summary, our results illustrate the difficulty to correlate serum IGFBP-3 levels with prostate cancer.

The effects of IGFBP-3 levels are very likely exceeded by locally produced IGFBP-3 in the prostate.

In addition, we observed that the stroma contributes significantly to IGFBP-3 levels in the prostate and in prostate cancer. This is a newly described mechanism that may be of great importance in understanding the biological effects of IGFBP-3 on epithelial cells. IGFBP-3 is up-regulated in local prostate cancer, presumably due to the activation of the stroma surrounding the tumor by TGF- $\beta$  and other factors. Further research is needed to elucidate the role of the stromal-epithelial interaction in modulating the bioavailability and activity of IGFBP-3 in the prostate, and to determine the impact of this phenomenon on the regulation of the IGF growth factor axis in tumor biology.

### ACKNOWLEDGMENTS

We thank Gabi Dobler for culture of primary and immortalized cells, Judith Kätzler for collection of ejaculate samples, Heidi Hübl for performing microdissections, Stephan Geley and Lukas A. Huber for providing the confocal microscope, and Pidder Jansen Dürr for providing the human recombinant IGFBP-3. Our special thanks to Iris E. Eder for constructive discussion and for proofreading the manuscript. This work was supported by the Cell Proliferation and Cell Death in Tumors (SFB021) project of the Austrian Research Foundation and the EU FP6 project named PRIMA (FP6-504587).

### REFERENCES

- Jemal A, Murray T, Ward E, Samuels A, Tiwari RC, Ghafoor A, Feuer EJ, Thun MJ. Cancer statistics, 2005. *CA Cancer J Clin* 2005; 55(1):10–30.
- Tuxhorn JA, Ayala GE, Rowley DR. Reactive stroma in prostate cancer progression. *J Urol* 2001;166(6):2472–2483.
- Sung SY, Chung LW. Prostate tumor-stroma interaction: Molecular mechanisms and opportunities for therapeutic targeting. *Differentiation* 2002;70(9–10):506–521.
- Rowley DR. What might a stromal response mean to prostate cancer progression? *Cancer Metastasis Rev* 1998;17(4):411–419.
- Zhao H, Ramos CF, Brooks JD, Peehl DM. Distinctive gene expression of prostatic stromal cells cultured from diseased versus normal tissues. *J Cell Physiol* 2007;210(1):111–121.
- Severi G, Morris HA, MacInnis RJ, English DR, Tilley WD, Hopper JL, Boyle P, Giles GG. Circulating insulin-like growth factor-I and binding protein-3 and risk of prostate cancer. *Cancer Epidemiol Biomarkers Prev* 2006;15(6):1137–1141.
- Platz EA, Pollak MN, Leitzmann MF, Stampfer MJ, Willett WC, Giovannucci E. Plasma insulin-like growth factor-1 and binding protein-3 and subsequent risk of prostate cancer in the PSA era. *Cancer Causes Control* 2005;16(3):255–262.
- Li L, Yu H, Schumacher F, Casey G, Witte JS. Relation of serum insulin-like growth factor-I (IGF-I) and IGF binding protein-3 to risk of prostate cancer (United States). *Cancer Causes Control* 2003;14(8):721–726.
- Shi R, Berkel HJ, Yu H. Insulin-like growth factor-I and prostate cancer: A meta-analysis. *Br J Cancer* 2001;85(7):991–996.
- Chen C, Lewis SK, Voigt L, Fitzpatrick A, Plymate SR, Weiss NS. Prostate carcinoma incidence in relation to prediagnostic circulating levels of insulin-like growth factor I, insulin-like growth factor binding protein 3, and insulin. *Cancer* 2005;103(1): 76–84.
- Winter DL, Hanlon AL, Raysor SL, Watkins-Bruner D, Pinover WH, Hanks GE, Tricoli JV. Plasma levels of IGF-1, IGF-2, and IGFBP-3 in white and African-American men at increased risk of prostate cancer. *Urology* 2001;58(4):614–618.
- Chokkalingam AP, Pollak M, Fillmore CM, Gao YT, Stanczyk FZ, Deng J, Sesterhenn IA, Mostofi FK, Fears TR, Madigan MP, Ziegler RG, Fraumeni JF Jr, Hsing AW. Insulin-like growth factors and prostate cancer: A population-based case-control study in China. *Cancer Epidemiol Biomarkers Prev* 2001;10(5): 421–427.
- Stattin P, Bylund A, Rinaldi S, Biessy C, Dechaud H, Stenman UH, Egevad L, Riboli E, Hallmans G, Kaaks R. Plasma insulin-like growth factor-I, insulin-like growth factor-binding proteins, and prostate cancer risk: A prospective study. *J Natl Cancer Inst* 2000;92(23):1910–1917.
- Hwa V, Oh Y, Rosenfeld RG. The insulin-like growth factor-binding protein (IGFBP) superfamily. *Endocr Rev* 1999;20(6): 761–787.
- Jones JL, Clemmons DR. Insulin-like growth factors and their binding proteins: Biological actions. *Endocr Rev* 1995;16(1): 3–34.
- Monti S, Proietti-Pannunzi L, Sciarra A, Lolli F, Falasca P, Poggi M, Celi FS, Toscano V. The IGF axis in prostate cancer. *Curr Pharm Des* 2007;13:719–727.
- Rajah R, Valentinis B, Cohen P. Insulin-like growth factor (IGF)-binding protein-3 induces apoptosis and mediates the effects of transforming growth factor-beta1 on programmed cell death through a p53- and IGF-independent mechanism. *J Biol Chem* 1997;272(18):12181–12188.
- Butt AJ, Firth SM, King MA, Baxter RC. Insulin-like growth factor-binding protein-3 modulates expression of Bax and Bcl-2 and potentiates p53-independent radiation-induced apoptosis in human breast cancer cells. *J Biol Chem* 2000;275:39174–39181.
- Boyle BJ, Zhao XY, Cohen P, Feldman D. Insulin-like growth factor binding protein-3 mediates 1 alpha,25-dihydroxyvitamin d(3) growth inhibition in the LNCaP prostate cancer cell line through p21/W AF1. *J Urol* 2001;165:1319–1324.
- Liu B, Lee KW, Anzo M, Zhang B, Zi X, Tao Y, Shiry L, Pollak M, Lin S, Cohen P. Insulin-like growth factor-binding protein-3 inhibition of prostate cancer growth involves suppression of angiogenesis. *Oncogene* 2007;26(12):1811–1819.
- Bhattacharyya N, Pechhold K, Shahjee H, Zappala G, Elbi C, Raaka B, Wiench M, Hong J, Rechler MM. Nonsecreted insulin-like growth factor binding protein-3 (IGFBP-3) can induce apoptosis in human prostate cancer cells by IGF-independent mechanisms without being concentrated in the nucleus. *J Biol Chem* 2006;281(34):24588–24601.
- Silha JV, Sheppard PC, Mishra S, Gui Y, Schwartz J, Dodd JG, Murphy LJ. Insulin-like growth factor (IGF) binding protein-3 attenuates prostate tumor growth by IGF-dependent and IGF-independent mechanisms. *Endocrinology* 2006;147(5):2112–2121.
- Kojima S, Mulholland DJ, Ettinger S, Fazli L, Nelson CC, Gleave ME. Differential regulation of IGFBP-3 by the androgen receptor in the lineage-related androgen-dependent LNCaP and

- androgen-independent C 4-2 prostate cancer models. *Prostate* 2006;66:971–986.
24. Peng L, Wang J, Malloy PJ, Feldman D. The role of insulin-like growth factor binding protein-3 in the growth inhibitory actions of androgens in LNCaP human prostate cancer cells. *Int J Cancer* 2007;122(3):558–566.
  25. Janssen JA, Wildhagen MF, Ito K, Blijenberg BG, Van Schaik RH, Roobol MJ, Pols HA, Lamberts SW, Schroder FH. Circulating free insulin-like growth factor (IGF)-I, total IGF-I, and IGF binding protein-3 levels do not predict the future risk to develop prostate cancer: Results of a case-control study involving 201 patients within a population-based screening with a 4-year interval. *J Clin Endocrinol Metab* 2004;89:4391–4396.
  26. Oliver SE, Holly J, Peters TJ, Donovan J, Persad R, Gillatt D, Pearce A, Hamdy FC, Neal DE, Gunnell D. Measurement of insulin-like growth factor axis does not enhance specificity of PSA-based prostate cancer screening. *Urology* 2004;64:317–322.
  27. Miyata Y, Sakai H, Hayashi T, Kanetake H. Serum insulin-like growth factor binding protein-3/prostate-specific antigen ratio is a useful predictive marker in patients with advanced prostate cancer. *Prostate* 2003;54:125–132.
  28. Haese A, Graefen M, Palisaar J, Huland E, Huland H. Serum markers for early detection and staging of prostate cancer. Status report on current and future markers. *Urolog A* 2003;42(9):1172–1187.
  29. Culig Z, Hoffmann J, Erdel M, Eder IE, Hobisch A, Hittmair A, Bartsch G, Utermann G, Schneider MR, Parczyk K, Klocker H. Switch from antagonist to agonist of the androgen receptor bicalutamide is associated with prostate tumour progression in a new model system. *Br J Cancer* 1999;81(2):242–251.
  30. Umekita Y, Hiiipakka RA, Kokontis JM, Liao S. Human prostate tumor growth in athymic mice: Inhibition by androgens and stimulation by finasteride. *Proc Natl Acad Sci USA* 1996;93(21):11802–11807.
  31. Pfeil K, Eder IE, Putz T, Ramoner R, Culig Z, Ueberall F, Bartsch G, Klocker H. Long-term androgen-ablation causes increased resistance to PI3K/Akt pathway inhibition in prostate cancer cells. *Prostate* 2004;58(3):259–268.
  32. Cronauer MV, Eder IE, Hittmair A, Sierek G, Hobisch A, Culig Z, Thurnher M, Bartsch G, Klocker H. A reliable system for the culture of human prostatic cells. *In Vitro Cell Dev Biol Anim* 1997;33(10):742–744.
  33. Corvin S, Bosch ST, Maneschg C, Bartsch G, Klocker H. An in vitro model for videoimaging of human bladder smooth muscle cell contractions. *Urol Res* 2000;28(4):250–253.
  34. Kogan I, Goldfinger N, Milyavsky M, Cohen M, Shats I, Dobler G, Klocker H, Wasyluk B, Voller M, Aalders T, Schalken JA, Oren M, Rotter V. hTERT-immortalized prostate epithelial and stromal-derived cells: An authentic in vitro model for differentiation and carcinogenesis. *Cancer Res* 2006;66(7):3531–3540.
  35. Schmidt U, Fuessel S, Koch R, Baretton GB, Lohse A, Tomasetti S, Unversucht S, Froehner M, Wirth MP, Meye A. Quantitative multi-gene expression profiling of primary prostate cancer. *Prostate* 2006;66(14):1521–1534.
  36. Huggett J, Dheda K, Bustin S, Zumla A. Real-time RT-PCR normalisation; strategies and considerations. *Genes Immun* 2005;6(4):279–284.
  37. Arya M, Shergill IS, Williamson M, Gommersall L, Arya N, Patel HR. Basic principles of real-time quantitative PCR. *Expert Rev Mol Diagn* 2005;5(2):209–219.
  38. Reiner A, Neumeister B, Spona J, Reiner G, Schemper M, Jakesz R. Immunocytochemical localization of estrogen and progesterone receptor and prognosis in human primary breast cancer. *Cancer Res* 1990;50(21):7057–7061.
  39. Liao Y, Abel U, Grobholz R, Hermani A, Trojan L, Angel P, Mayer D. Up-regulation of insulin-like growth factor axis components in human primary prostate cancer correlates with tumor grade. *Hum Pathol* 2005;36(11):1186–1196.
  40. Tennant MK, Thrasher JB, Twomey PA, Birnbaum RS, Plymate SR. Insulin-like growth factor-binding protein-2 and -3 expression in benign human prostate epithelium, prostate intra-epithelial neoplasia, and adenocarcinoma of the prostate. *J Clin Endocrinol Metab* 1996;81(1):411–420.
  41. Miyata Y, Sakai H, Kanda S, Igawa T, Hayashi T, Kanetake H. Expression of insulin-like growth factor binding protein-3 before and after neoadjuvant hormonal therapy in human prostate cancer tissues: Correlation with histopathologic effects and biochemical recurrence. *Urology* 2004;63(6):1184–1190.
  42. Aksoy Y, Aksoy H, Bakan E, Atmaca AF, Akcay F. Serum insulin-like growth factor-I and insulin-like growth factor-binding protein-3 in localized, metastasized prostate cancer and benign prostatic hyperplasia. *Urol Int* 2004;72(1):62–65.
  43. Bach LA. The insulin-like growth factor system: Towards clinical applications. *Clin Biochem Rev* 2004;25:155–164.
  44. Phillips LS, Pao CI, Villafuerte BC. Molecular regulation of insulin-like growth factor-I and its principal binding protein, IGFBP-3. *Prog Nucleic Acid Res Mol Biol* 1998;60:195–265.
  45. Tennant MK, Thrasher JB, Twomey PA, Birnbaum RS, Plymate SR. Insulin-like growth factor-binding proteins (IGFBP)-4, -5, and -6 in the benign and malignant human prostate: IGFBP-5 messenger ribonucleic acid localization differs from IGFBP-5 protein localization. *J Clin Endocrinol Metab* 1996;81(10):3783–3792.
  46. Thrasher JB, Tennant MK, Twomey PA, Hansberry KL, Wettlaufer JN, Plymate SR. Immunohistochemical localization of insulin-like growth factor binding proteins 2 and 3 in prostate tissue: Clinical correlations. *J Urol* 1996;155(3):999–1003.
  47. Cohen P, Peehl DM, Baker B, Liu F, Hintz RL, Rosenfeld RG. Insulin-like growth factor axis abnormalities in prostatic stromal cells from patients with benign prostatic hyperplasia. *J Clin Endocrinol Metab* 1994;79(5):1410–1415.
  48. Cohen P, Graves HC, Peehl DM, Kamarei M, Giudice LC, Rosenfeld RG. Prostate-specific antigen (PSA) is an insulin-like growth factor binding protein-3 protease found in seminal plasma. *J Clin Endocrinol Metab* 1992;75(4):1046–1053.